JOURNAL OF GEOPHYSICAL RESEARCH, VOL. 99, NO. C7, PAGES 14,321–14,338, JULY 15, 1994

Concurrent measurements of the directional spectra of microseismic energy and surface gravity waves

T. Nye and T. Yamamoto

Division of Applied Marine Physics, Rosensteil School of Marine and Atmospheric Sciences, University of Miami, Florida

Abstract. This paper presents concurrent measurements of surface wave directional spectra and double-frequency, long-wave microseisms. Long-wave energy rapidly develops during periods of shifting winds which create bidirectional sea states. Theoretically, nonlinear sum interactions of opposing wavenumber vectors of approximately the same frequency create long-wave energy at twice the frequency, which is only slightly attenuated in shallow water. Bidirectional sea states have been found using a buried ocean bottom seismometer measuring system from which the long wave energy has been measured at double frequencies. This system was incorporated into the Office of Naval Research sponsored Sources of Ambient Microseismic Ocean Noise (SAMSON) experiment for 3 months off the Army Corps of Engineers' Field Research Facility near Duck, North Carolina in the fall of 1990. Four working sensors produced directional spectra results from nearly 22 gigabytes of recorded data, which was collected 2 km offshore of the FRF under 12–13 m of water and approximately 1 m of sediment. Because of the insignificant attenuation the measured energy levels of the double frequency microseisms at the seafloor are of the same order of magnitude as the single-frequency, surface wave energy induced seafloor motion. Various data sets were analyzed that confirmed Longuet-Higgins' theory, which proposes that the propagation direction of double-frequency microseisms occurs in the direction of the vector sum of the opposing single-frequency seas.

Introduction

In September 1990, an Office of Naval Research (ONR) sponsored multiinstitutional project named Sources of Ambient Microseismic Ocean Noise (SAMSON) began. The University of Miami's Geoacoustic Laboratory's (UM/GAL) contribution to this experiment was a six-point ocean bottom seismometer (OBS)/pressure array located 2 km offshore of the Army Corps of Engineers Field Research Facility (FRF) at Duck, North Carolina. The individual OBS/pressure units measured the directional spectra of the surface gravity waves as single-point measuring devices, as the array was not tuned to the gravity wave frequency band. An array of bottom-mounted pressure sensors (FRF units in 8 m water depth) is used as a comparison device to confirm the surface spectra [*Nye and Yamamoto*, 1993].

The UM/GAL array was tuned to measure energy in the 'double-frequency' microseism band. *Longuet-Higgins* [1950] proposed that microseisms may develop as a result of bidirectional seas with similar frequencies and opposing directions, creating a standing wave and causing pressure fluctuations, which in turn excite the seafloor at twice the frequency of the opposing wave trains. These 'double-frequency' oscillations can be propagated to great depths. This paper finds bidirectional sea states where the opposing vectors of the seas created the double-frequency microseismic energy. It will be shown that this energy is created when wind shifts cause the seas to bifurcate. The high-frequency gravity waves are the first to move to the direction of the new wind, creating double-frequency microseism energy above 0.6 Hz. As the gravity wave energy that transfers to the new wind direction moves to lower-frequency bands, the double-frequency energy also moves to lower-frequency bands following the 2:1 ratio. After the sea state has stabilized to a unidirectional field, the double-frequency energy may remain for hours before diminishing altogether. *Herbers and Guza* [1992] have shown that the microseismic energy is also pronounced during unidirectional, high-energy sea states. The double-frequency microseisms are interface waves, allowing for measurements of power, point coherence/phase between vertical and horizontal seismometers, and spatial coherence/phase between units in the array.

Double-frequency microseisms are generated on the seafloor because of pressure fluctuations caused by nonlinear interactions between opposing wave trains of approximately the same frequency. Sum interactions and difference interactions occur between wave trains with $f_1 \approx f_2$ and $\mathbf{k}_1 \approx -\mathbf{k}_2$. The difference interaction produces energy at double frequency and double wavenumber (Stoke's second harmonic), which, because of the depth of the study area, do not reach the seafloor in the frequency band of interest (0.3–1.0 Hz). The sum interaction produces double-frequency oscillations with the wavenumber approximately equal to zero (*Miche* [1944] from *Herbers and Guza* [1991]). This very long wavelength energy endures almost no attenuation in 12–13 m water depths and thus produces pressure fluctuations on the seafloor at twice the frequency of the opposing surface waves. *Herbers and Guza* [1991] show that the interaction coefficient (C) between the opposing seas decreases if the separation of the bidirectionality becomes less than 180° or if

Paper number 94JC00612.
0148-0227/94/94JC-00612$05.00

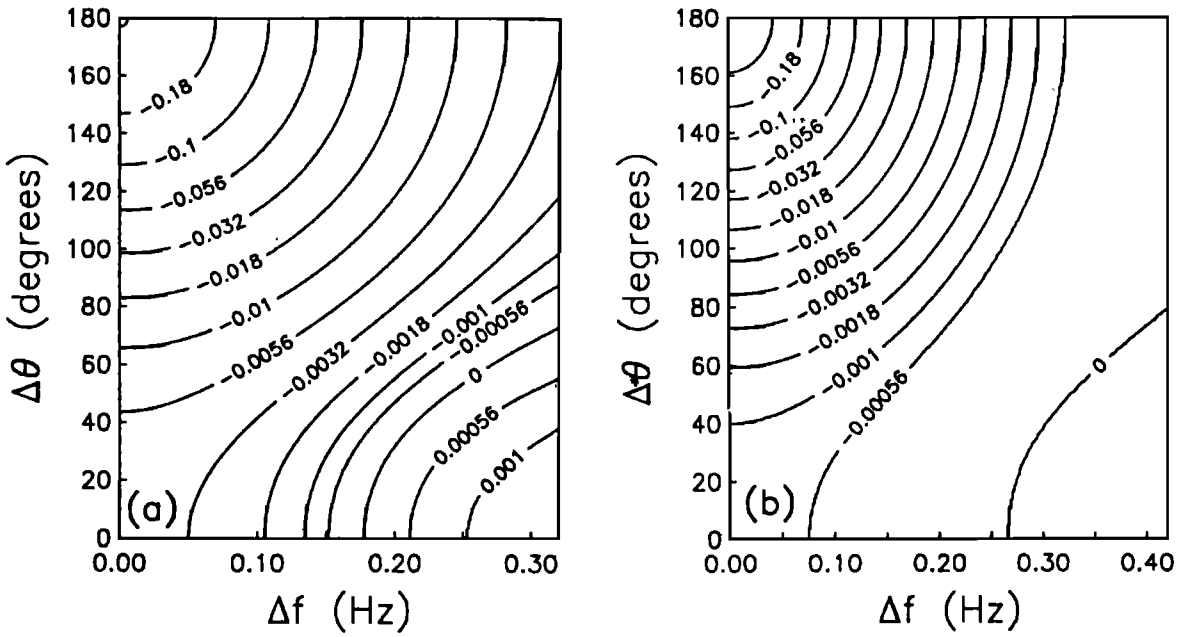

Figure 1. Nonlinear interaction coefficient (C) in 13 m depth as a function of $\Delta\theta$ and Δf for (a) f_0 equal to 0.4 Hz where C = -0.32 m^{-1} at $\Delta\theta = 180°$ and $\Delta f = 0.0$ and (b) f_0 equal to 0.5 Hz where C = -0.50 m^{-1} at $\Delta\theta = 180°$ and $\Delta f = 0.0$. [*Herbers and Guza*, 1991].

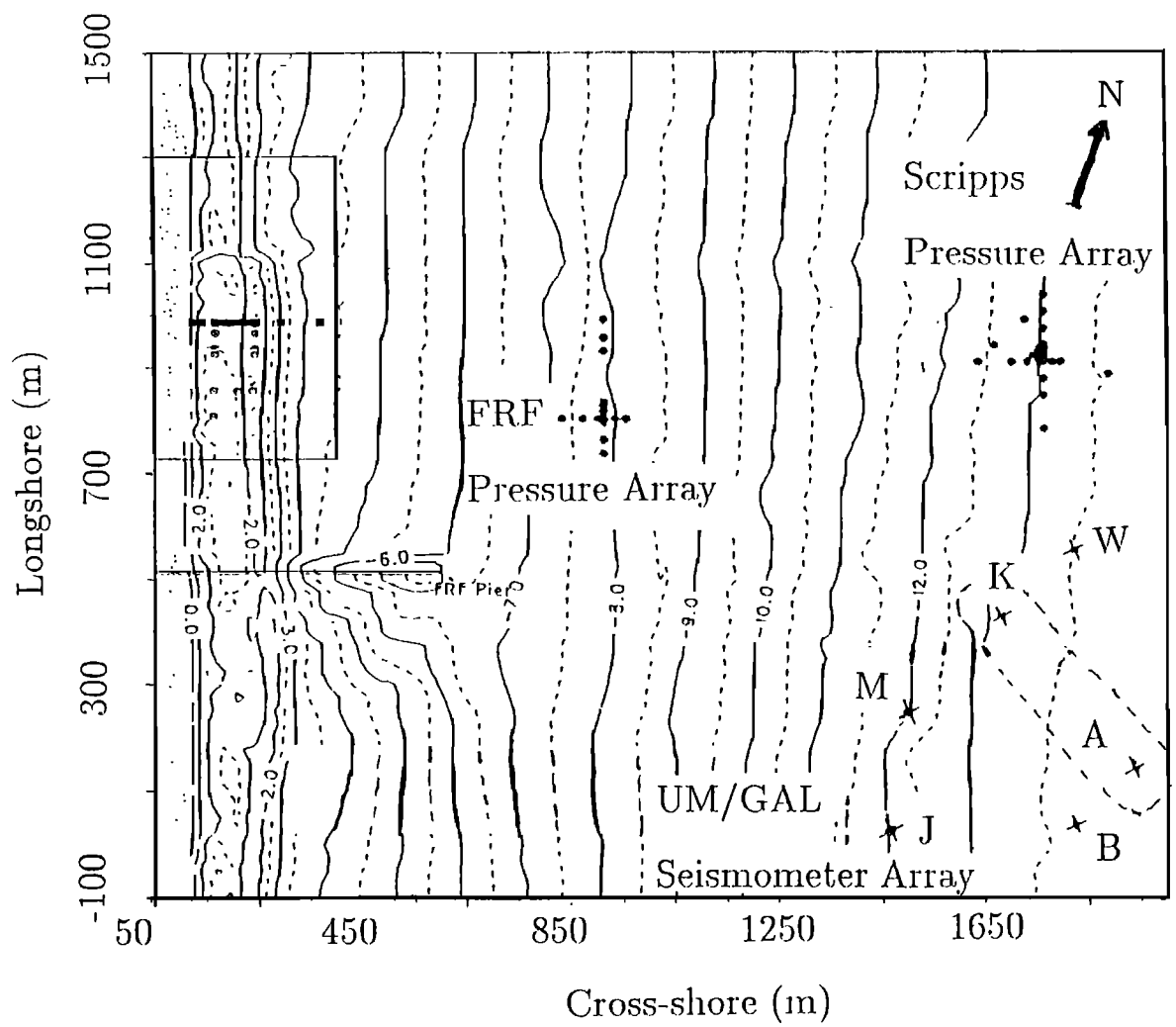

Figure 2. Map of the Sources of Ambient Micro-seismic Ocean Noise (SAMSON) experimental site.

Table 1. Instrument Positions

Instrument	Cross-Shore, m	Longshore, m	Depth, m
Joanna	1460	27	12.2
Miyuki	1502	205	13.7
Ayshe	1942	130	13.7
Beth	1817	46	12.8
Karen	1675	455	13.7
Wendy	1810	571	13.4

Table 2. Instrument Bearings

Instrument	Roll, deg	Pitch, deg	Heading, deg Azimuth
Joanna	0.0	2.0	112
Miyuki	3.5	2.0	82
Ayshe	4.2	3.0	135
Beth	7.5	3.0	107
Karen	5.5	0.4	285
Wendy	7.0	3.0	55

the frequency varies between the seas (see Figure 1). They calculated that C becomes a tenth of its maximum value if $\Delta\theta$ decreases to 90° in 13 m of water at $f_0 = 0.4$ Hz (this depth is similar to the SAMSON site and 0.4 Hz double-frequency fluctuations are common). The coefficient also decreases to a tenth of its maximum if $\Delta f = 0.2$ Hz when $f_0 = 0.4$ Hz. The frequency which is approximately double the frequency of the opposing seas is f_0. The difference in frequency between the opposing seas is Δf and is centered at f_0. With $f_0 = 0.5$ Hz, the calculated values reduced to 1% of the maximum for $\Delta\theta = 90°$ or $\Delta f = 0.25$ Hz. Double-frequency energy often will be produced from opposing seas which are not 180° apart or of exactly the same frequency; however, for energy to develop in the higher-frequency bands, the seas must truly oppose and be of the same frequency.

The nonlinear interactions cause pressure fluctuations on the bottom which propagate away from the generation area at speeds much greater than the speed of the gravity waves. *Longuet-Higgins* [1950] proposed that if the two arms of the opposing seas were not 180° apart, the long-wave, double-frequency oscillation would propagate away from the generation area in the direction of the vector sum of the two seas.

SAMSON Experiment

The 1990 experiment offshore of the Corps of Engineers FRF at Duck, North Carolina (Figure 2) was part of the multiinstitutional Sources of Ambient Microseismic Ocean Noise (SAMSON) experiment. UM/GAL's contribution to this experiment was a near-shore (2 km) seismometer array consisting of six ocean bottom seismometers with pressure sensors (OBSs). Some other components of SAMSON are shown in Figure 2, including the FRF's 12-point, bottom-mounted pressure array, which was used to find the directional spectra of the surface waves. Located offshore of this array and to the north of the UM/GAL array, was Scripps Institute of Oceanography's 32-sensor, bottom-mounted pressure array. This array has a small aperture to measure surface wave directional spectra and a larger aperture to also find double-frequency microseism wavenumber vectors. The other instruments shown but not labeled are surf zone current meters. Duck, North Carolina, lies midway between Cape Hatteras and Virginia Beach on North Carolina's outer bank. This group of instruments represented SAMSON's near shore components. There were also offshore microseismic measurements and a large-aperture, land-based seismometer array.

The deployment of the UM/GAL array, which was tuned to find the directional spectra of double-frequency microseisms (array spacing being too large to find the directional spectra of gravity waves using array methods) began on September 6, 1990. Three kilometers of armored, 1-inch-diameter coaxial cable was deployed offshore of the FRF. This cable contained three breakout points for instrument placement at the far end, 600 m in, and 1200 m in. At these points, three secondary armored, 5/8-inch-diameter, 200-m-long coaxial cables were deployed. In Table 1 the six instrument positions are given in meters cross-shore and longshore (x and y, respectively) from the origin of the FRF coordinate system, latitude 36°10'38.77"N and longitude 75°45'0.28"W. The six instrument packages were buried using divers and a hydraulic pump jet system which liquefied the sediment allowing the instruments to settle to depths of 1 m. The accelerometers were leveled by hand. Instrument tilts and headings (direction of horizontal seismometer labeled 'transverse') are given in Table 2.

The instrument package consisted of three separate units. The first was an accelerometer unit containing three orthog-

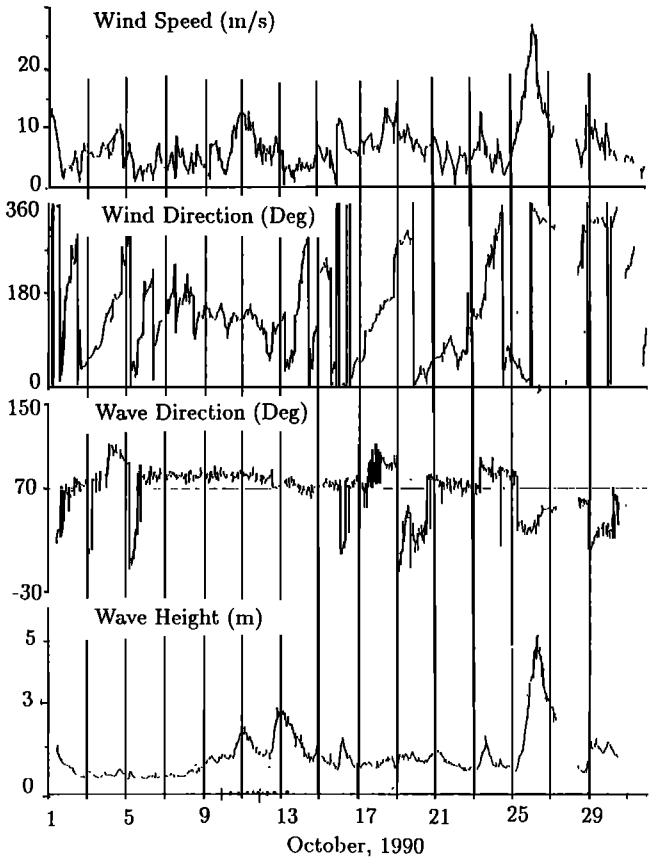

Figure 3. Wind and wave data for the month of October, 1990 collected from the Field Research Facility's pier gauges.

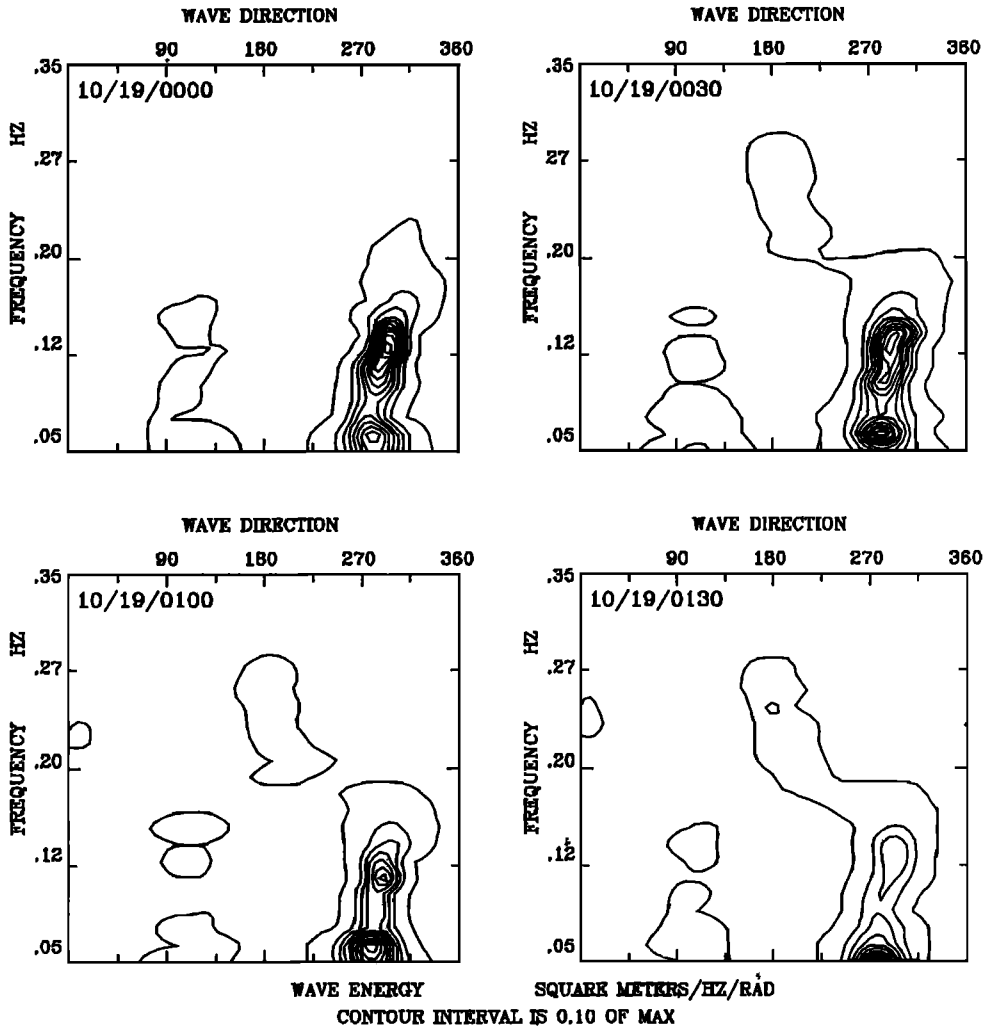

Figure 4. Directional spectra results from the 1990 SAMSON experiment for the Joanna unit for four 30-minute time periods beginning October 19, 0000, 0030, 0100, and 0130 UT, respectively.

onally mounted seismometers (Teledyne-Geotech models S-750 or S-510), a compass (Aanderaa model 1248), and two pendulum tiltmeters (Sperry model 02383-01). The accelerometer unit was cased in an aluminum alloy cylinder (diameter, 30.5 cm; height, 25.5 cm) which was approximately of neutral density in sediment to provide adequate coupling with the sea bottom. This housing is buried, with its axis oriented vertically, to a depth of 1 m. The second unit in the instrument package was an electronics container which consisted of an aluminum alloy housing (diameter, 23 cm; height, 48 cm) containing instrumental amplifiers, filters, digitizers, and digital multiplexer electronics. This unit served as a junction between the seismometer unit, the pressure sensor, and the electromechanical cable to shore. The final piece of the package was the pressure sensor (Precision Measurements Engineering model 109). The electronics housing and the pressure sensor were buried to depths of approximately 0.5 m to protect them from fishery activity.

During a period of repair to an instrument umbilical by cable manufacturers, a short to seawater apparently caused inductors in two instruments (Ayshe and Karen) to overheat. These inductors were on the digital multiplexer boards built by Teledyne-Geotech and could not be replaced by the start date of the SAMSON project. Therefore these two units were out of commission and the experiment began with a four-point accelerometer array. Data acquisition began on October 9 and concluded on January 3, 1991.

Results

Wind and wave amplitude and direction are given in Figure 3 for the month of October 1990. Wind measurements were collected by anemometers on the FRF pier, while wave measurements are made by the FRF's array (wave height is given as significant wave height). This figure was produced by FRF personnel. A major wind shift occurred on October 18 while the wind speed remained high (8–15 m/s). The wind veered clockwise from northeast to northwest from the morning of October 17 to the morning of October 19. Most of the shift comes in the late evening of October 18. FRF instruments show that the mean wave direction shifted 120° (first coming from east and then coming from north-northwest) on the morning of October 19.

Figures 4 and 5 show the evolution of these seas as measured by the unit labeled Joanna. These plots represent the directional spectra of the surface gravity waves using a

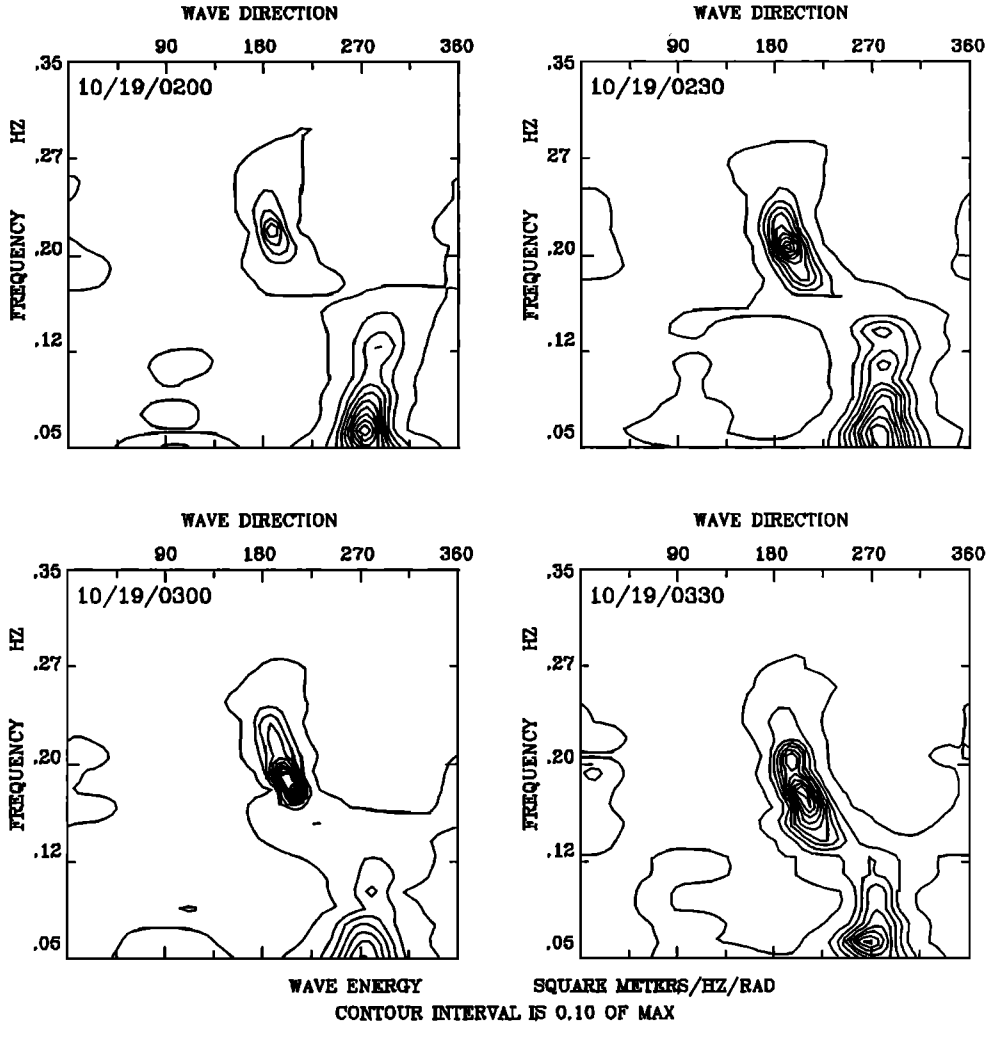

Figure 5. Directional spectra results from the 1990 SAMSON experiment for the Joanna unit for four 30-minute time periods beginning October 19, 0200, 0230, 0300, and 0330, respectively.

point, three-axis measurement (two directions of horizontal acceleration and pressure), and the maximum entropy analysis. The single-point measuring device favorably compared to FRF's bottom-mounted array of pressure sensors [*Nye*, 1992; *Nye and Yamamoto*, 1993]. The FRF plots are averaged over too long a time period (3 hours) to adequately show the evolving seas. The x axes of Figures 4 and 5 represent the direction of wave propagation from north. The FRF pier extends into the ocean at 70° perpendicular to the shore, therefore waves which perpendicularly approach the beach propagate toward 250°. The y axes are the wave frequency in Hz increasing from 0.05 Hz to 0.35 Hz. Any wave information at frequencies higher than 0.25 Hz is suspect owing to the shallow water cutoff (water depth is about 12 m). Figure 4 represents the directional spectra for the Joanna unit for four 30-minute time periods October 19, 0000 UT–October 19, 0130 UT from upper left to lower right respectively. The first plot (October 19, 0000 UT) shows wave energy propagating toward 280° at 0.06 Hz and 300° at 0.13 Hz. By 0030 UT, another sea begins to develop at 0.2–0.27 Hz, propagating toward 180°. This energy slowly builds through the next hour (graphs 10/19/0100 and 10/19/0130) as the 0.13 Hz/300° energy diminishes. Figure 5 displays the four 30-minute segments of the directional spectra of the Joanna unit from beginning at October 19, 0200 UT to beginning at October 19, 0330 UT from upper left to lower right. During the first segment (0200 UT) the waves propagate toward 180°/0.22 Hz and 270°/0.06 Hz. The following three time frames indicate wave energy building in the southerly direction and abating in the westerly direction. The peak frequency in the wind generated spectra moves from 0.22 Hz to 0.17 Hz during this interval. A closer inspection of graph 10/19/0230 reveals a bidirectional sea state at 0.16 Hz with the opposing vectors being 210° and 280°. This corresponds to an interaction coefficient of approximately -0.01 m^{-1} using Figure 1 with f_0 at 0.4 Hz (which is slightly high for this data). This is approximately 3% of the nonlinear interaction one could expect from truly opposing seas at exactly the same frequency. It will be shown that this is sufficient to create long-wave energy that impinges the seafloor to the same order of magnitude as the attenuated surface waves themselves. The vector sum of these two seas resides at 245°, which is the direction that the resulting double-frequency energy should propagate with a frequency near 0.32 Hz.

Figure 6 displays the power spectra for the Joanna unit's

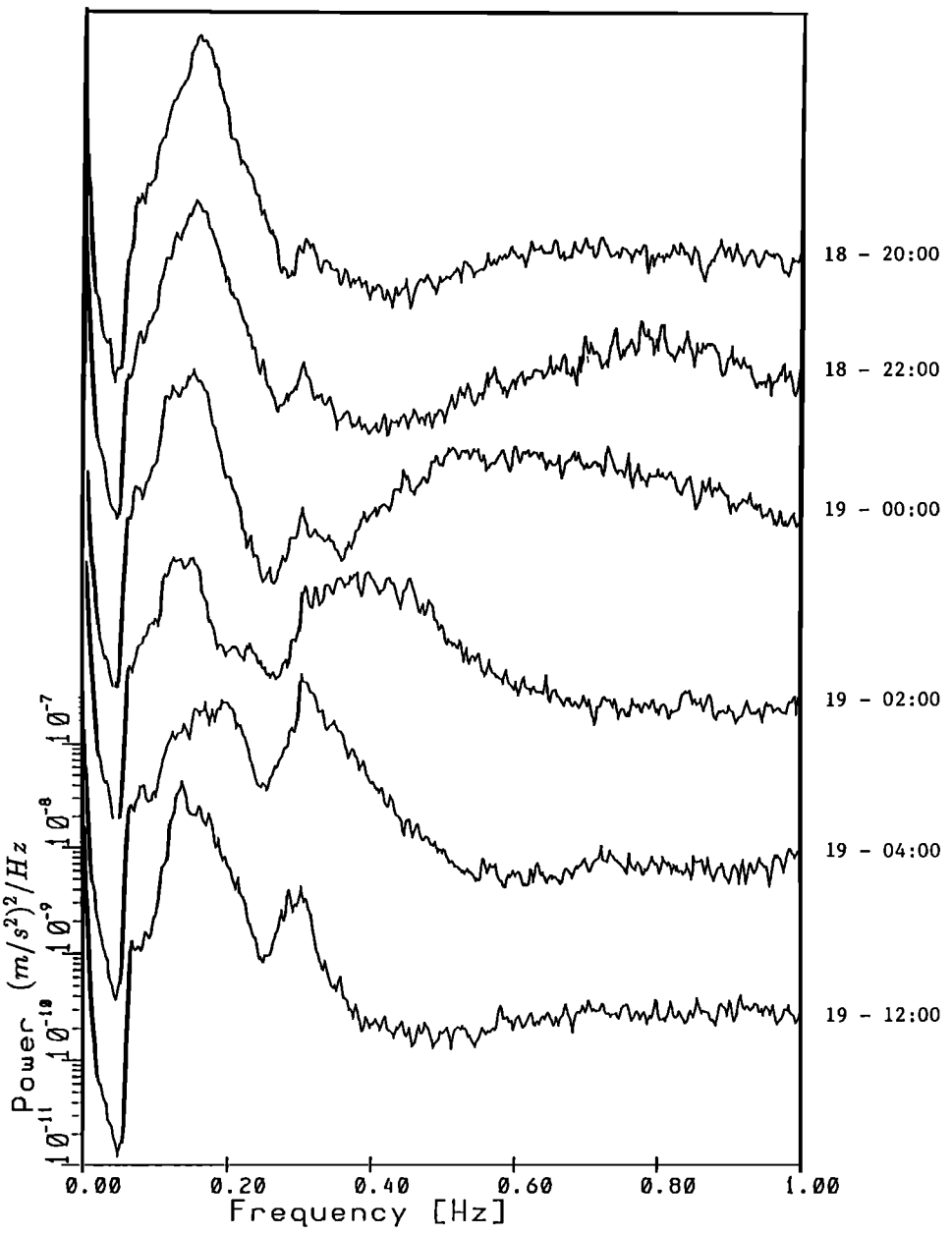

Figure 6. Vertical seismometer power spectra versus frequency for the Joanna unit time periods October 18, 1990, 2000 UT to October 19, 1990, 1200 UT.

vertical seismometer for 2-hour averaged data sets (October 18, 1990, 1800–2000 UT through October 19, 1990, 1000–1200 UT). This figure is given in frequency versus log power $((m/s^2)^2/Hz)$ with the October 18, 1800 UT data set displayed at the top. Because the wind is veering during this time one expects the high-frequency band to first develop wave energy aligned with the new wind. *Young et al.* [1987] indicate that there is a strong frequency dependence in directional relaxation with the low-frequency wind-driven waves lagging behind the high-frequency waves. However, there is more than one environmental factor working during this period. The wind has begun to shift by October 18, 1800 UT, but the waves which follow this shift at high frequencies are not yet measurable by bottom-mounted sensors. The small peak at 0.3 Hz on the first line of Figure 6 is long-wave microseismic energy which is not generated by opposing seas because the spectrum is unidirectional at 0.15 Hz during this time segment. This energy is suspected to be long-wave energy because the spatial coherence is good and the spatial phase is steady between instruments far enough apart (up to 650 m) to safely rule out the possibility of it being gravity wave energy (to be shown later in Figures 13–16).

By 1800–2000 UT the high-frequency energy begins to produce double-frequency microseisms centered at f_0 = 0.80 Hz. The single-frequency (0.4 Hz) surface wave energy that presumably creates this peak is still immeasurable at the bottom, however the 0.3-Hz long-wave energy is still apparent during this segment of data. For the 0.8-Hz energy to be locally generated (a valid assumption given the weather conditions and the spectral plots that follow), it could be produced only as long-wave, double-frequency energy caused by the 'sum' nonlinear interactions of opposing wave

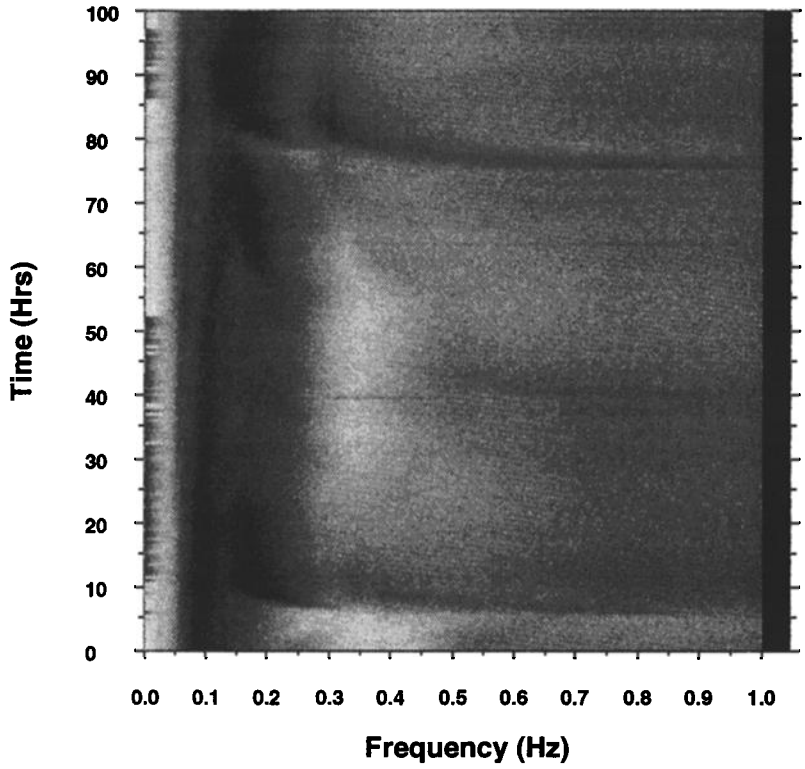

Figure 7. Vertical seismometer power spectra versus frequency for the Joanna unit time periods October 15, 1800 UT to October 19, 2000 UT.

trains. The single-frequency gravity waves at 0.4 Hz are attenuated by an inverse cosh (kd) term of the order of 10^{-12} and cannot affect the bottom. The Stoke's nonlinear interactions are double-frequency, half-wavelength and are attenuated even more. The long-wave energy attenuates very little, which causes the double-frequency microseism peak to be higher at the seafloor than the peak of the waves which created it. During the following 2 hours the peak of the long-wave energy moves toward lower frequencies and becomes broad band but centered around 0.6 Hz. This indicates that lower-frequency wave trains are becoming bidirectional, which is in agreement with the findings of *Young et al.* [1987]. This data set (October 18, 2200 UT–October 19, 0000 UT) labeled 10/18/22:00 indicates a 0.3-Hz peak which could be a combination of the long-wave microseisms and the new wind-driven surface waves which slightly affect the bottom at 0.3 Hz. The directional spectra plot does not yet notice this surface wave energy, however. The next vertical seismometer power spectra line, 19-00:00 (October 19, 0000–0200 UT), corresponds to the bidirectional seas which are represented in Figure 4. The surface waves show two directions of propagation near 0.2 Hz. Figure 6 indicates a strong double-frequency peak centered at 0.4 Hz for the 19-02:00 data set. Where the previous microseismic energy could only be assumed to be double frequency, for this data set it has been shown that bidirectional seas exist at half the frequency of the intense 0.4-Hz microseismic peak, corroborating the theory of Longuet-Higgins. In this time segment the gravity wave peak of the new wind energy begins to merge with the peak of the spectra. The double-frequency peak (centered at 0.4 Hz) is of the same order of magnitude as the spectral peak. During the following 10 hours the long-wave energy peak settles to approximately 0.3 Hz and narrows to a band width of less than 0.1 Hz. The energy level where the seas are bidirectional (0.15–0.2 Hz for these data sets) is very low, yet the energy this produces through nonlinear interactions is of the same order of magnitude on the seafloor as the peak of the spectra. The ocean acts as a natural filter in which very small amounts of long-wave energy can dominate the higher-frequency bands. In the deep ocean this long-wave, double-frequency energy is the major source of ambient noise in the 0.1–1.0 Hz frequency range because other wave-induced sources are attenuated to zero.

To understand the time evolution of the microseismic energy, a more detailed graph of the power spectra of the Joanna vertical seismometer signal is given in Figure 7. This figure shows spectral information from October 15, 1800 UT to October 19, 2000 UT for two hundred 30-minute intervals. The intensity ranges from 10^{-7} $(m/s^2)^2/Hz$ (black) to 10^{-12} $(m/s^2)^2/Hz$ (white). The x axis is frequency in hertz, while the y axis is time in hours, where October 15, 1800 UT is the zero hour. Therefore the time when it was shown that bidirectional seas existed in Figure 4, October 19, 0030 UT, is represented at 78.5 hours on this graph. The main features on this figure are the band of gravity wave energy from 0.05–0.3 Hz and the streaks of double-frequency energy at approximately 5 and 75 hours. While there is more energy in the frequency band above 0.5 Hz than was seen in other weeks, the two high-energy double-frequency features from 5–10 hours and 75–90 hours dominate this band. In Figure 7 the shift from high to low frequency of the passing event is

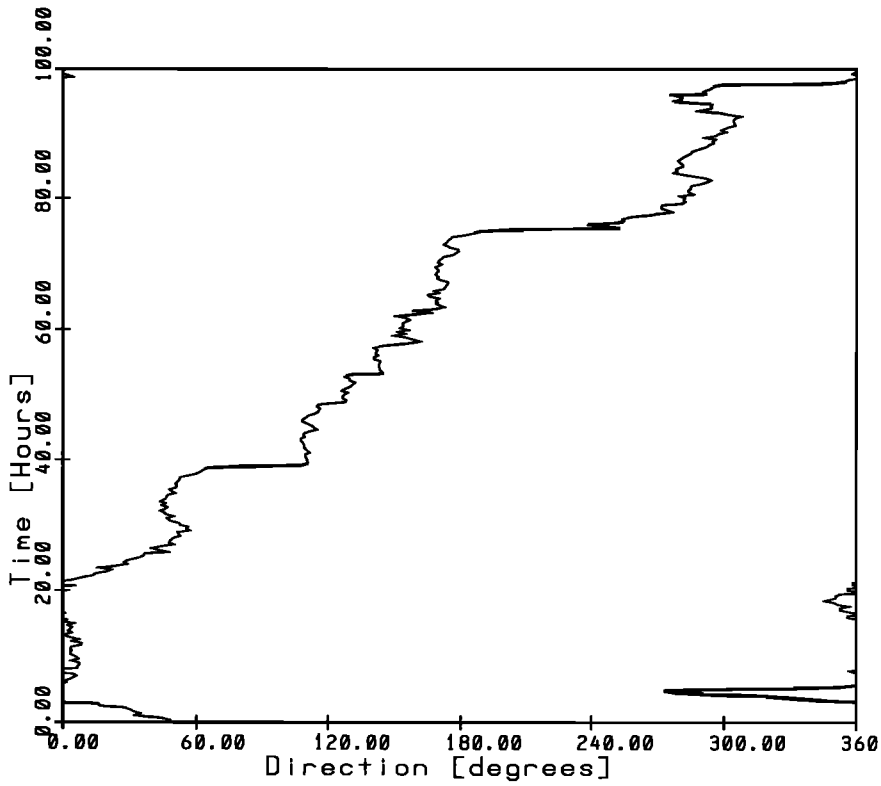

Figure 8. Wind data for October 15, 1800 UT to October 19, 2000 UT collected from the FRF's pier gauges.

readily apparent by the curved nature of the streak. The double-frequency energy increases dramatically at 75 hours at high frequencies, which is precisely when the wind begins to shift, as seen in Figure 8 (the same October wind conditions as in Figure 3 with the October 15, 1800 UT–October 19, 2000 UT data blown up to match Figure 7). As the wind shifts from southerly to northwesterly, the long-wave energy develops.

It is of interest to also look at the power spectra from horizontal units to inspect for differences from the vertical to the horizontal plane. Figure 9 displays the power spectra of the transverse seismometer of the Joanna unit for the same 100-hour time frame beginning October 15, 1800 UT. The energy scale for the vertical, transverse, and radial seismometers will remain constant (10^{-7} $(m/s^2)^2$/Hz to 10^{-12} $(m/s^2)^2$/Hz) throughout this paper. The energy measured by the transverse accelerometer closely matches that of the vertical and the events at 5 and 75 hours are clearly evident. Figure 10 depicts the same 100-hour data set beginning at October 15, 1800 UT for the power spectra of the radial seismometer in the Joanna instrument. Because this seismometer is oriented nearly parallel to shore, very little energy is measured during periods of onshore swell as seen between the twenty-fifth and seventy-fifth hours. The energy between 0.3 and 0.4 Hz near 70 hours now becomes apparent (it can also be seen in the vertical and transverse spectra, but stands out against the lower background energy in this figure). This energy exists well before the major wind shift at 75 hours and remains nearly unchanged until the double-frequency energy curve caused by the new bidirectional sea overwhelms it at approximately 79 hours.

One advantage to having a wide aperture array of OBS units buried at the SAMSON site was that spatial coherence and phase between instruments could be calculated. Figure 2 showed the relative positions of each instrument with respect to shore. Distances between instruments ranged from 183 m (Joanna–Miyuki) to 647 m (Joanna–Wendy). Figure 11 displays the spatial coherence and phase between midrange (≈400 m) units Joanna and Beth for the 2-hour data set terminating at October 18, 2000 UT. The gravity waves near 0.06 Hz are coherent with respect to these instruments, with the double-frequency energy showing good coherence from 0.3 to approximately 0.7 Hz. According to Figure 6, energy in the frequency band 0.4–1.0 Hz was low compared to other frequency bands and also compared to later data sets; however, the coherence between instruments remains high. The wave energy from 0.3 to 0.35 Hz is also coherent. Figure 12 (October 19, 0200 UT) indicates an increase in coherence from approximately 0.65 to 0.90 for energy in the frequency band centered at 0.4 Hz (0.3–0.5 Hz). As the microseismic energy level increases in a frequency band, the coherence between instruments generally increases also.

In order to see more detail in the spatial coherence and phase, Figures 13–16 have been included. These figures show coherence and phase between instruments for 200 thirty-minute data sets beginning at October 15, 1800 UT. Figure 13 depicts the coherence between vertical seismometers in the Joanna and Beth units (separation distance, 400 m). The x axis represents frequency from 0.0 to 1.0 Hz and the y axis is time in hours where October 15, 1800 UT is the zero hour. The scale ranges from a coherence of 0.0 (white) to 1.0 (black). Although some coherence exists throughout

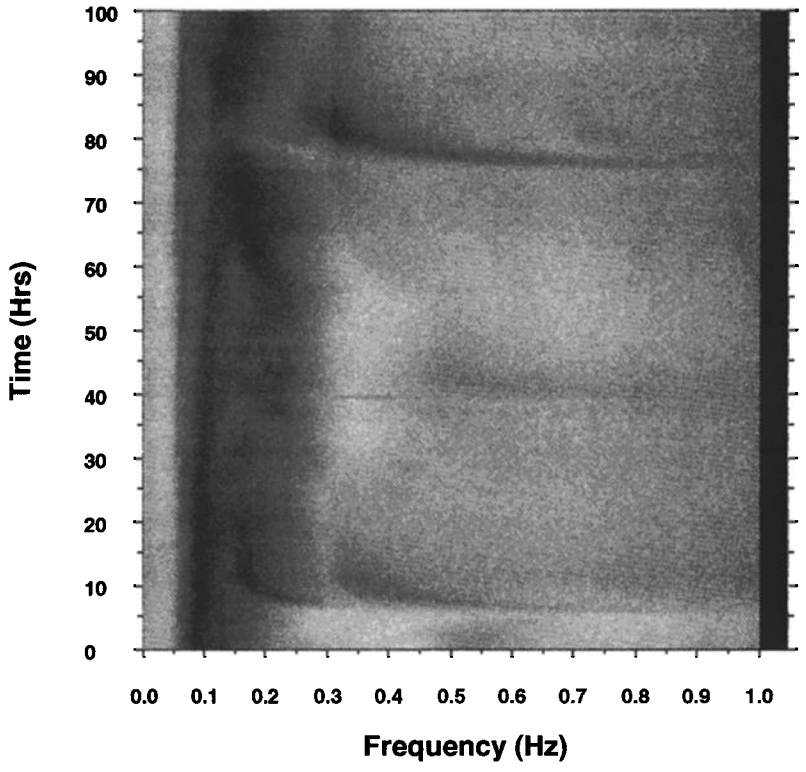

Figure 9. Transverse seismometer power spectra versus frequency for the Joanna unit time periods October 15, 1800 UT to October 19, 2000 UT.

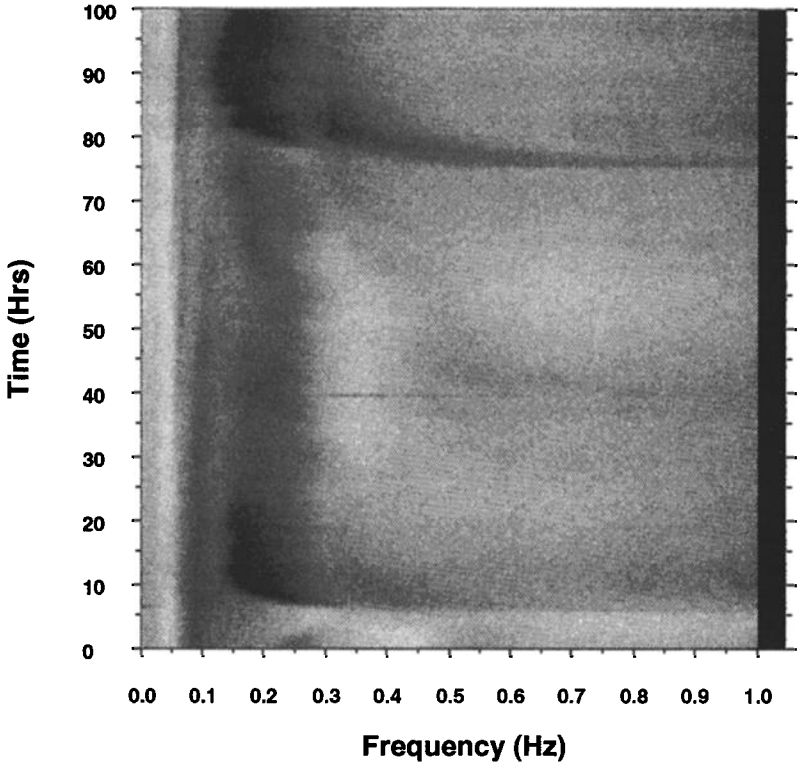

Figure 10. Radial seismometer power spectra versus frequency for the Joanna unit time periods October 15, 1800 UT to October 19, 2000 UT.

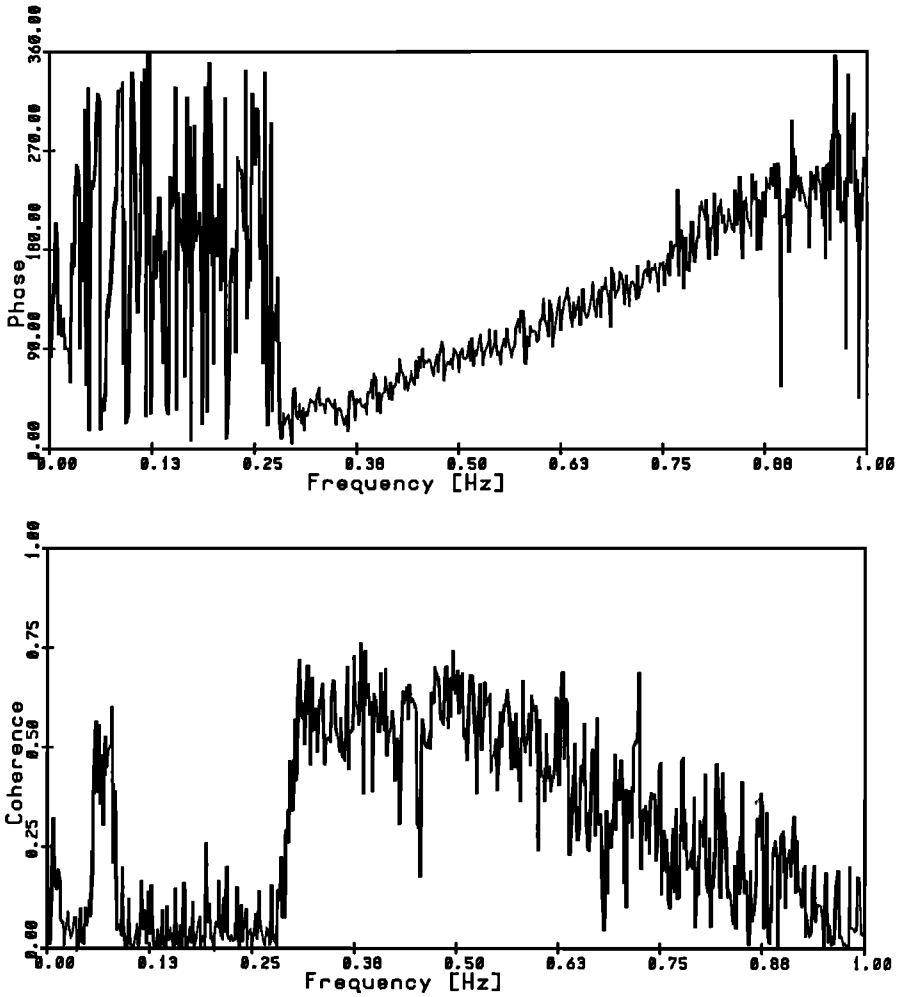

Figure 11. Phase and coherence between the vertical seismometers in the Joanna and Beth units for the 2-hour data set terminating at October 18, 2000 UT.

the 4-day period, the two measured bidirectional events at 5–10 hours and 75–90 hours stand out. The shorter-wavelength gravity wave band (0.1–0.3 Hz) has zero coherence across this distance. However, the swell energy at 0.06 Hz is slightly coherent (0.06-Hz waves have a wavelength of 400 m in this water depth). The long-wave, double-frequency microseismic energy shows good coherence down to nearly 0.25 Hz at 85 hours. At 75 hours (October 18, 2100 UT), there is good spatial coherence at 0.3 Hz which is an indication that the energy measured in this frequency band in Figures 6, 7, 9, and 10 during the late evening of October 18 is not due to the relatively short wavelength gravity waves. Figure 14 shows the spatial phase between the Joanna and Beth vertical seismometers for the 100-hour time frame starting at October 15, 1800 UT. Phase between signals range from 0° (white) to 359° (black). This plot indicates that the phase between these two signals is steady throughout the 4-day period. The phase is near 0° in the 0.3 Hz range and increases slightly with increasing frequency to 0.75 Hz, which is an indication of higher-frequency microseisms having shorter wavelengths. At the swell frequency (near 0.05 Hz) and to a lesser extent the gravity wave frequencies (0.1–0.25 Hz) the phase is banded, indicating wavelengths shorter than the separation distance repeating all phases with increasing frequency. Between 70 and 75 hours and at 0.3 Hz, however, the phase is stable, which again is an indication of long-wave propagation. The two bidirectional sea events at 5–10 and 75–90 hours are noticed as a slight change toward lower phase. It follows that the direction in which these events propagate is not wildly different than the low-energy propagation of the entire 4 days.

Figure 15 shows the coherence between the Joanna vertical seismometer and the Miyuki vertical seismometer (separation distance = 180 m). Although the units are much closer, because they lie roughly parallel to shore, the swell energy near 0.05 Hz is not coherent, as it was in Figure 13 between Joanna and Beth. The two strongly coherent events lie between 0–10 hours and 75–90 hours. The most notable feature being the curve to lower frequency (0.25 Hz) of the strongly coherent 75–90 hour event. Figure 16 displays the spatial phase between the same two instruments. The scale now ranges from −180° (white) to +180° (black) with the 0° phase being indicated by the grey of the border. The phase between these two signals is generally zero with very little frequency dependence. The banded nature of the gravity wave frequency band is again apparent as is the hourglass shape on the left-hand side as the event passes to lower frequencies. The dark streak at 75 hours indicates a positive

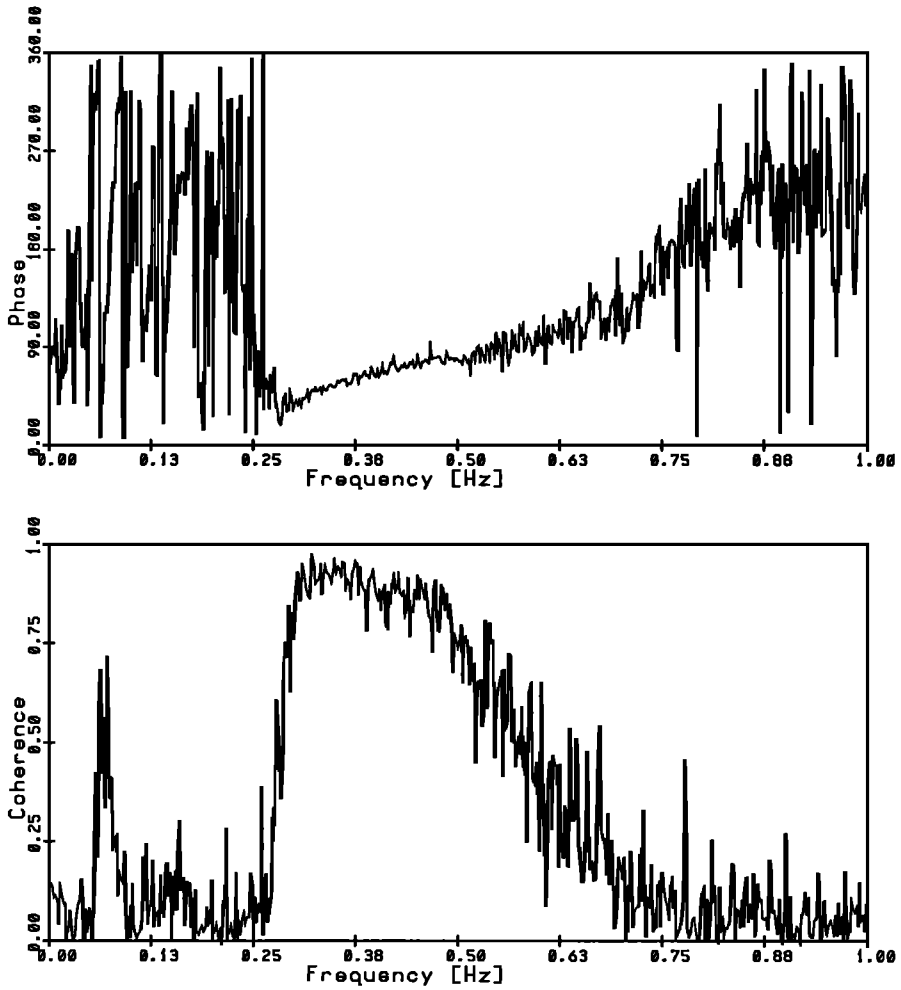

Figure 12. Coherence and phase between the vertical seismometers in the Joanna and Beth units for the 2-hour data set terminating at October 19, 0200 UT.

phase swing as the double frequency event passes by. Also, the energy at 0.3 Hz and 75 hours is characterized by steady phase, again indicating long-wave energy. The general nature of the spatial coherence and phase indicates that finding the directional spectra of this long-wave energy is possible, and given the very high coherence, the spectra plots should have good resolution to the limits of the response function of the array.

The array of four OBS units (Joanna, Miyuki, Beth, and Wendy) is used to estimate the directional spectra of seafloor, double-frequency microseisms during the SAMSON experiment. An ideal array would require an infinite number of cross spectra between instruments with varying spatial lags. Because only four units are available the response of this array has significant sidelobes and a broad primary lobe [*Nye*, 1992]. The response, however, is sufficient to show propagation directions of the long-wave energy in order to complete the analysis of microseism generation due to bidirectional sea states. In his thesis, *Goodman* [1990] describes the maximum likelihood method (MLM) algorithm used to find the following spectra. He also suggested that beam forming be used instead of MLM in cases where the cross spectrum is noisy. Beam forming was tried and found unfavorable in comparison to MLM's resolution (the cross spectra show high coherence, low noise for these data). Therefore the long-wave directional spectra estimates are calculated by MLM.

It has previously been estimated that the propagation direction of the long-wave energy should be 245° for 0.32-Hz energy during the 30-minute time frame starting at October 19, 0230 UT. This was based upon Longuet-Higgins' theory that the arms of the bidirectional sea add to produce the propagation direction of the double frequency energy. Figure 17 presents the directional spectra of this double frequency energy for four frequency bands. From upper left to lower right the estimated spectra are centered around f_0 equal to 0.3, 0.4, 0.5, and 0.6 Hz. The spectrum is averaged over $\Delta f = 0.02$ Hz for f_0 equal to 0.3 and 0.4 Hz, and $\Delta f = 0.04$ Hz for f_0 equal to 0.5 and 0.6 Hz because the lower frequencies tended to have higher coherence (less noise) than the higher frequencies. Each graph displays wave direction of propagation versus phase speed (meters per second). The algorithm varies phase speed (c) and calculates wavenumber (k) as $k = 2\pi f_0/c$. The directional spread is found for each value of c to find the most likely direction and speed. For small c, and therefore small wavelength, spatial aliasing can occur in the higher-frequency graphs. The contours are normalized by the maximum of each graph and

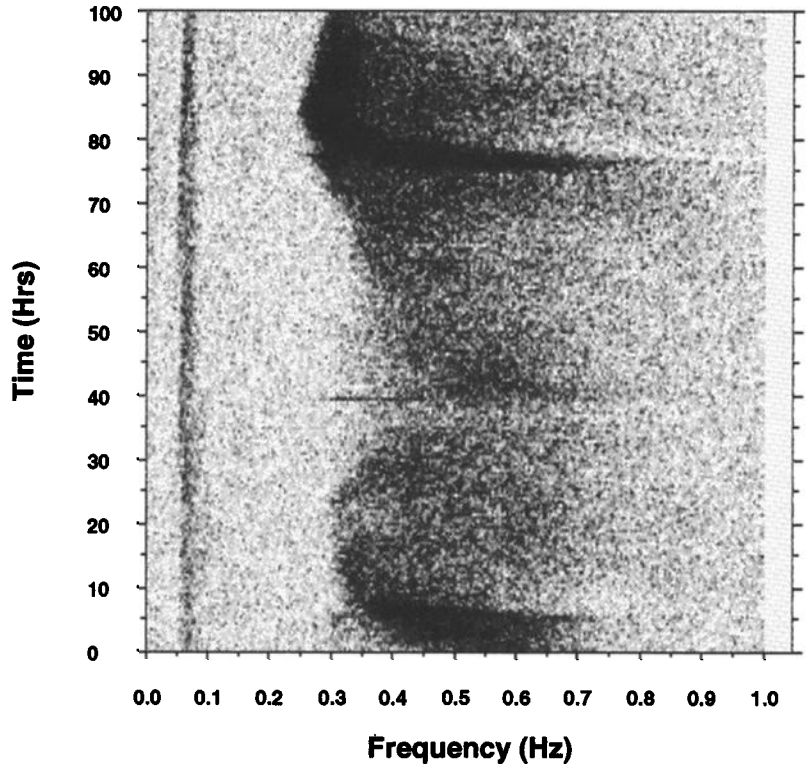

Figure 13. Spatial coherence between Joanna and Beth's vertical seismometers (400 m apart) versus frequency for time periods October 15, 1800 UT to October 19, 2000 UT.

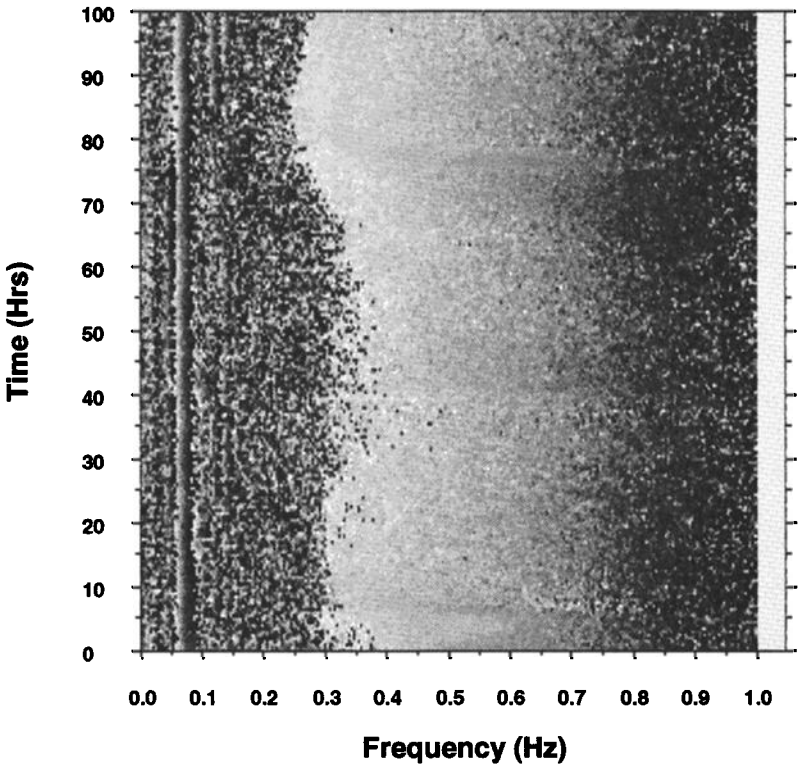

Figure 14. Spatial phase between Joanna and Beth's vertical seismometers (400 m apart) versus frequency for time periods October 15, 1800 UT to October 19, 2000 UT.

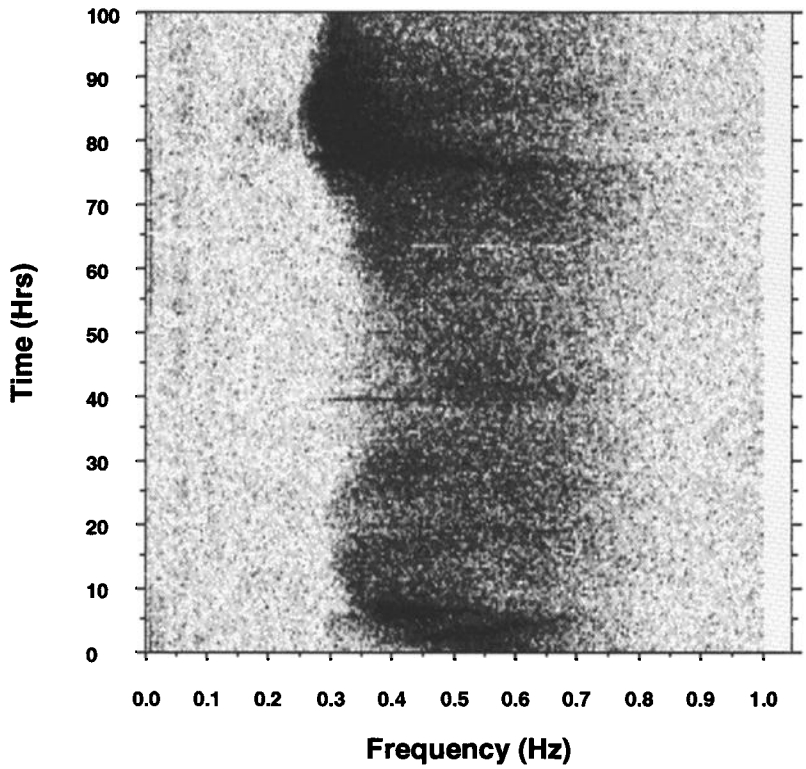

Figure 15. Spatial coherence between Joanna and Miyuki's vertical seismometers (180 m apart) versus frequency for time periods October 15, 1800 UT to October 19, 2000 UT.

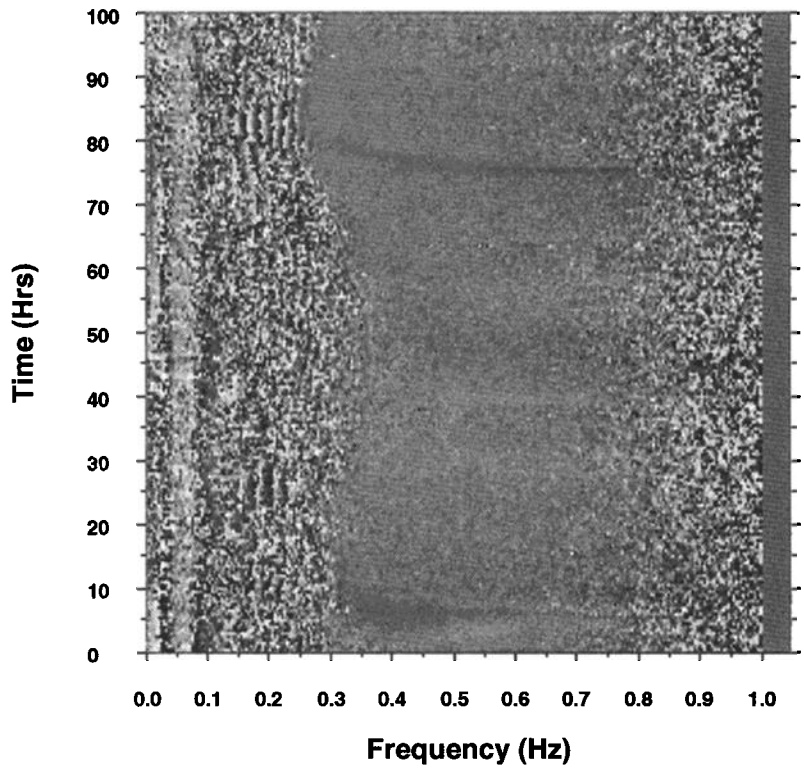

Figure 16. Spatial phase between Joanna and Miyuki's vertical seismometers (180 m apart) versus frequency for time periods October 15, 1800 UT to October 19, 2000 UT.

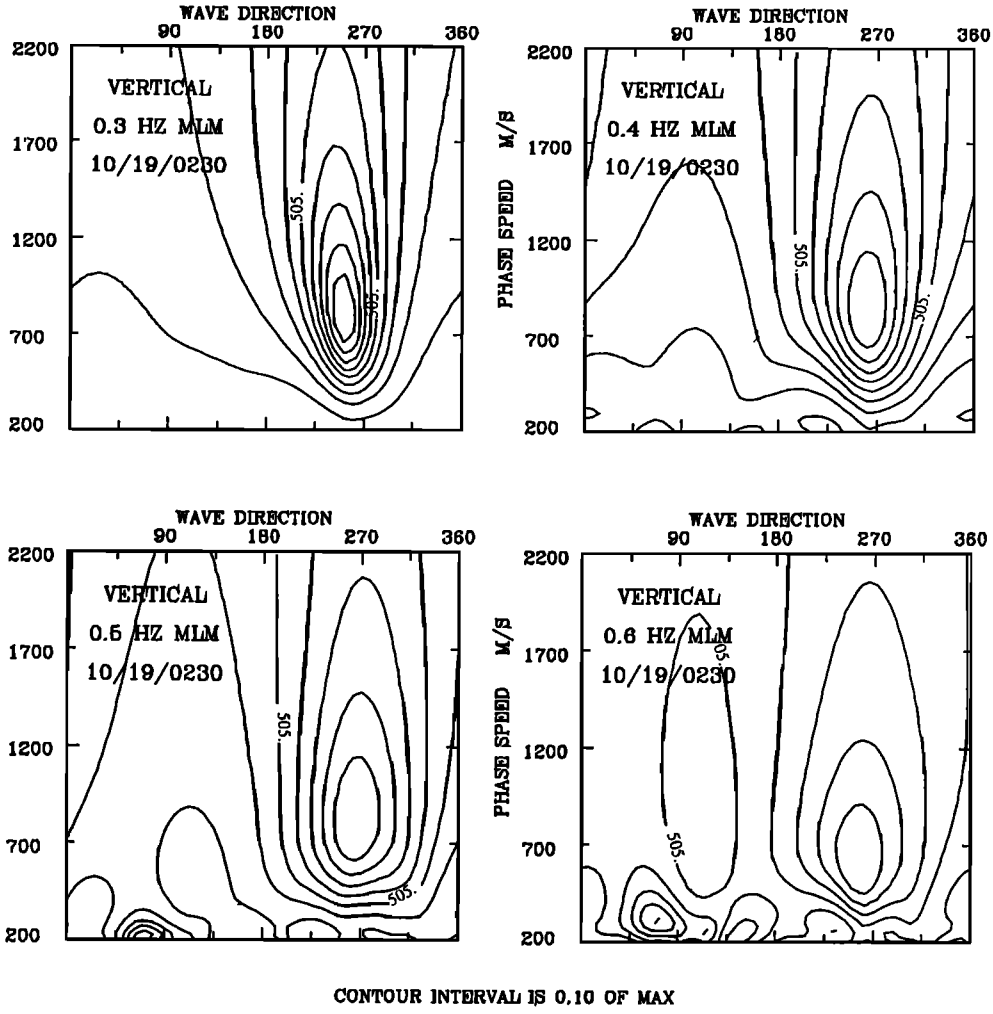

Figure 17. Double-frequency directional spectra estimation from the vertical seismometer four-point array using the maximum likelihood method during the 30-minute data set beginning at October 19, 0230 UT for frequency bands centered at 0.3, 0.4, 0.5, and 0.6 Hz, respectively, from upper left to lower right.

the contours are given in tenths of the maximum. Figure 17 indicates that the most likely propagation direction of the 0.3 Hz energy is 250° at a phase speed of 850 m/s, which closely agrees with the vector sum of the opposing seas which was estimated at 245°. The next frequency investigated was 0.4 Hz which shows a maximum at 260°, 900 m/s but is less sharp than the 0.3-Hz case. The higher-frequency cases, 0.5 Hz and 0.6 Hz, show maxima at 270°, 900 m/s and 260°, 700 m/s, respectively, with the resolution decreasing in each case. Some spatial aliasing can be seen at very low phase speeds on these graphs, which can be ignored. This time period represents the double-frequency event, as it was well established in the gravity wave band. However, investigating further back in the progression of this event, where the bidirectional sea state cannot be measured at the ocean floor but only assumed, the directional spectra graphs of Figure 18 are produced. This figure shows four frequency bands, 0.3, 0.4, 0.5, and 0.6 Hz with the same band widths as the Figure 17. In this case, at October 18, 2200 UT, the resolution in all four frequency bands are approximately equal. The 0.5 Hz and the 0.6 Hz bands at 230°, 650 m/s and 245°, 650 m/s, respectively, most likely are the summation of the opposing vectors of the new wind and old wind-driven energy. The more southerly direction of propagation coincides with the north winds, which would most likely create high-frequency surface waves traveling toward 180°. At the lower frequencies is the result of the long-wave energy from 0.3 to 0.4 Hz, which exists before the wind shift event but whose generation mechanism has not been accounted for. The peaks of the 0.3 and 0.4 Hz energy are 270°, 1100 m/s and 260°, 850 m/s, respectively. There is a gradual change between the 0.3 Hz graph presented here and the one from Figure 17, which occurs 4.5 hours later.

In order to substantiate the results from the October 19 event, another data set is investigated. The ocean surface directional spectra plotted in Figure 19 are a representation of the November 29, 1990, 1000 to 1200 UT data from the Joanna unit. The x axis describes direction of wave propagation in azimuthal direction from north, and the y axis is frequency from 0.05–0.35 Hz. The wave energy is normalized by the maximum of each plot and is given in square meters per hertz per radian where the contour interval is tenths of the maximum. The graphs represent 30-minute averages of the data beginning at November 29, 1000, 1030,

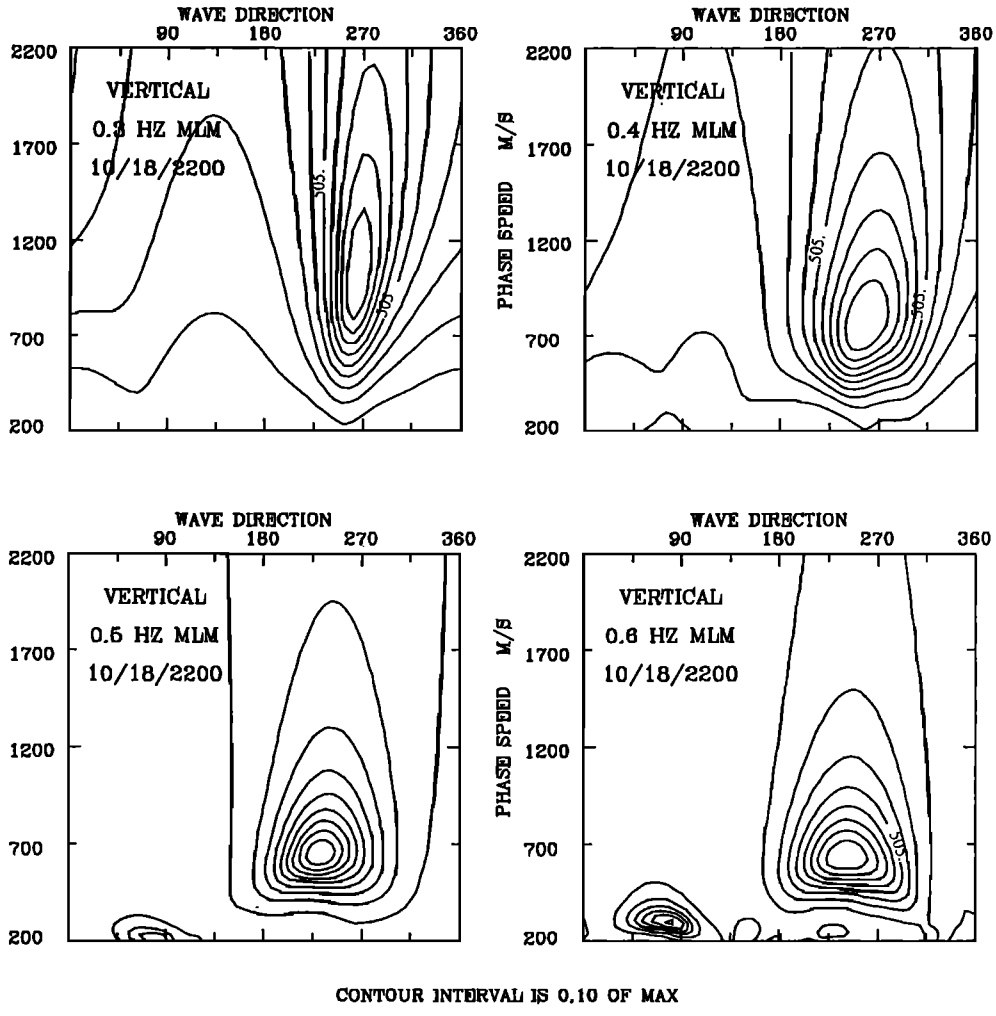

Figure 18. Double-frequency directional spectra estimation from the vertical seismometer four-point array using the maximum likelihood method during the 30-minute data set beginning at October 18, 2200 UT for frequency bands centered at 0.3, 0.4, 0.5, and 0.6 Hz, respectively, from upper left to lower right.

1100, and 1130 UT from upper left to lower right, respectively. The sea state propagating toward 180° near 0.27 Hz in the 11/29/10:00 plot increases in energy, moves to lower frequency, and shifts slightly west of south in the following 1.5 hours. The old energy includes a long-period swell to 270°, 0.06 Hz and a wind-driven peak at 300°, 0.12 Hz, both of which diminish throughout the time frame. An approximate summation of wavenumber vectors for each of the four time periods indicates vectors toward 235° at 0.5 Hz, 250° at 0.36 Hz, 255° at 0.3 Hz, and 245° at 0.28 Hz, respectively.

Figure 20 shows the power spectra of the vertical seismometer of the Joanna unit for the 4-day period beginning at November 28, 1000 UT. The x axis represents frequency from 0 to 1 Hz and the y axis is time in hours. The time frame discussed in the previous figure, November 29, 1000–1200 UT is represented as 24 to 26 hours. The intensity again ranges from 10^{-7} $(m/s^2)^2/Hz$ (black) to 10^{-12} $(m/s^2)^2/Hz$ (white). The double-frequency nature of this energy is clearly evident in Figure 20 as two curves, one with twice the frequency of the other, appear at 24 hours. The wall of microseismic energy has a width of the order of the resolution of this diagram, which is 30 minutes. *Herbers and Guza* [1992] found the double-frequency energy to increase an order of magnitude in 16 minutes for this same data set.

The array of transverse seismometers is used to find the directional spectra of this double-frequency energy using the MLM algorithm. Figure 21 shows the directional spectra results for the microseism energy in four frequency bins centered at 0.3, 0.4, 0.5, and 0.6 Hz, respectively, from upper left to lower right for the 30-minute time period November 29, 1000 UT. The bin widths are 0.02 Hz around the 0.3 and 0.4 Hz cases and 0.04 Hz around the 0.5 and 0.6 Hz cases. The graphs are in wave direction of travel versus phase speed. The 0.3-Hz case shows little resolution at this time. The 0.4-Hz case indicates the direction of propagation to be 225° at 700 m/s. The 0.5-Hz bin gives 230° at 650 m/s and the 0.6-Hz bin gives 250° at 600 m/s. The 0.5-Hz graph has the tightest resolution and matches the prediction from the vector sum of the opposing seas to 5°. The final 30-minute data set in this period of interest (November 29, 1130 UT) is given in Figure 22. Here the 0.3-Hz frequency band indicates spectra at 255° at 900 m/s, which is within 10° of the predicted vector (the energy in this frequency band competes with the higher-frequency gravity waves and therefore

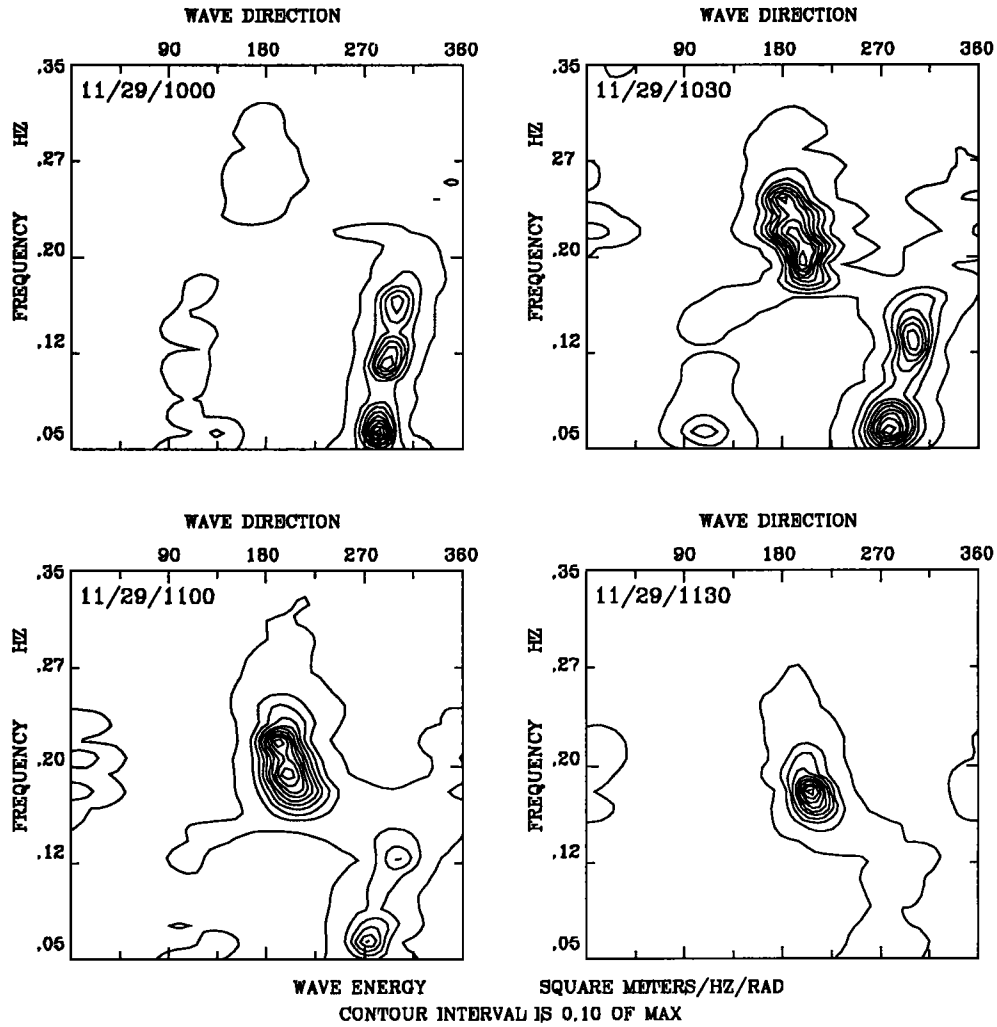

Figure 19. Ocean surface directional spectra results from the 1990 SAMSON experiment for the Joanna unit for four 30-minute time periods beginning November 29, 1000, 1030, 1100, and 1130 UT, respectively.

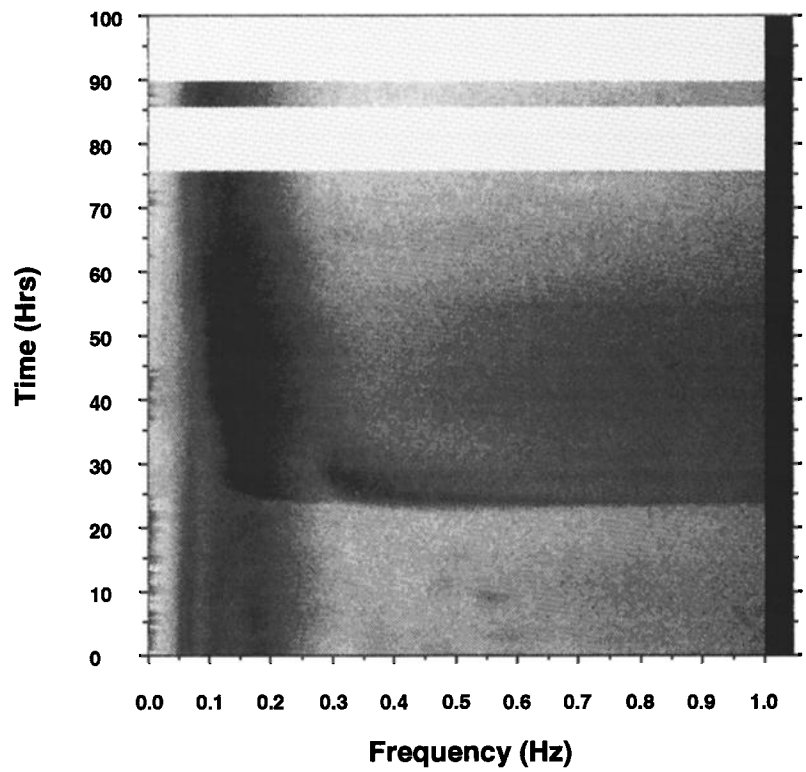

Figure 20. Vertical seismometer power spectra versus frequency for the Joanna unit time periods November 28, 1000 UT to December 2, 0200 UT.

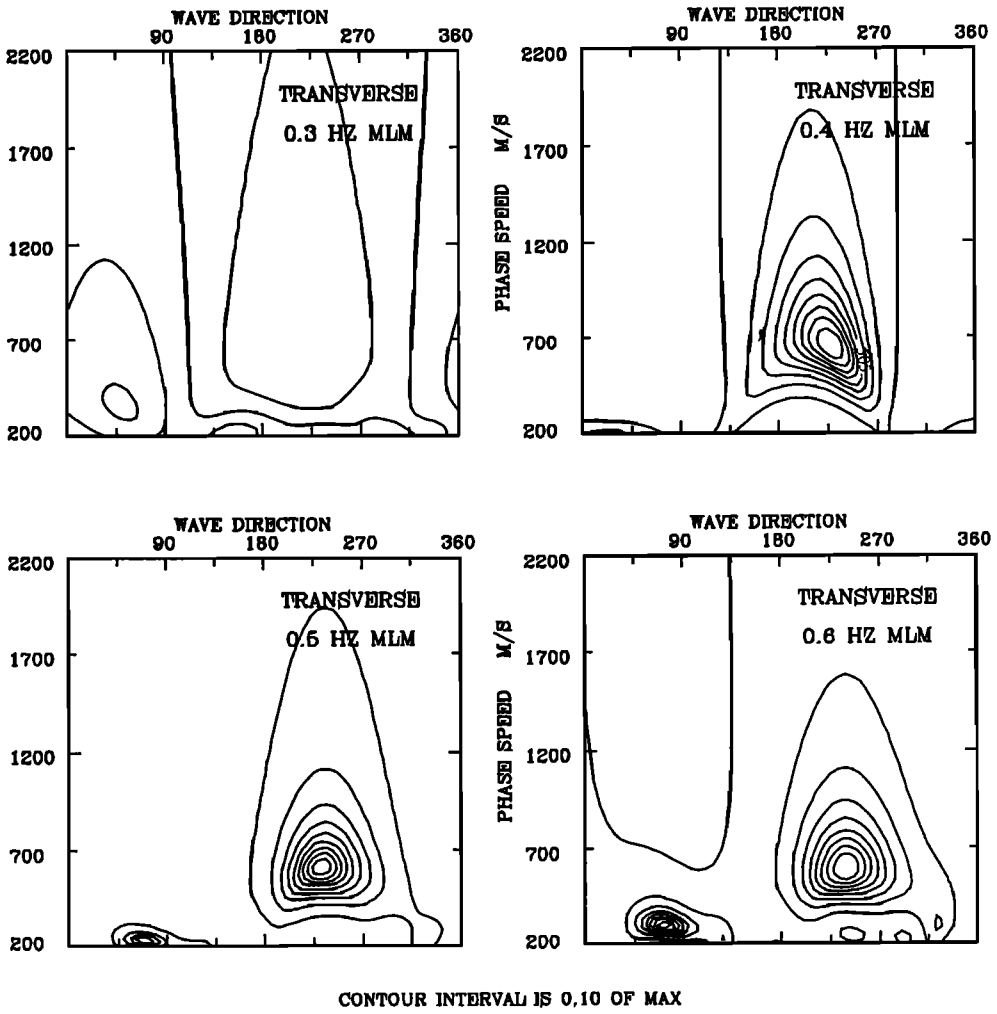

Figure 21. Double-frequency directional spectra estimation from the transverse seismometer four-point array using the maximum likelihood method during the 30-minute data set beginning at November 29, 1000 UT for frequency bands centered at 0.3, 0.4, 0.5, and 0.6 Hz, respectively, from upper left to lower right.

tends to have weaker resolution. The 0.4-Hz figure shows 245° at 700 m/s, the 0.5-Hz bin gives the same 245° at 700 m/s, and the 0.6-Hz bin shows 250° at 700 m/s. In general, the spectral peak moves from higher to lower frequency with time and to a more westerly direction, as was predicted by the bidirectional sea state. *Herbers and Guza* [1992] have also shown that the wavenumber vectors of the opposing arms of the bidirectional seas sum to a vector in the same direction as the direction of propagation of the long-wave, double-frequency energy in this data set.

Discussion and Conclusion

During the SAMSON experiment, concurrent measurements of surface wave directional spectra and double-frequency, long-wave microseisms were made. The results indicate that long-wave energy rapidly develops during periods of shifting winds which create bidirectional sea states. Theoretically, nonlinear sum interactions of opposing wavenumber vectors of approximately the same frequency create long-wave energy at twice the frequency, which is only slightly attenuated in shallow water. Bidirectional sea states have been found using the buried OBS measuring system, during which the long-wave energy has been measured at double frequencies. As the wind shifts, this energy forms at high frequencies and moves to lower frequencies following the single-frequency (surface wave) energy in a 2:1 ratio. Because of the insignificant attenuation the measured energy levels of the double-frequency microseisms at the seafloor are of the same order of magnitude as the single-frequency, surface wave energy induced seafloor motion. Indeed, very little energy needs to be directionally opposing to create long-wave energy at measurable levels, because this energy dominates the 0.4–1.0-Hz frequency bands in the water depths of the study area. All other locally generated sources of microseisms do not reach the bottom in this frequency band.

The double frequency microseism energy has been found to be coherent between vertical seismometers across the array with steady phase. Some coherence exists even during periods of low energy in the double-frequency band. However, the coherence increases dramatically during bidirectional sea events. The phase can also change during the event depending upon the direction of the double-frequency energy. The horizontally oriented seismometers also show good coherence with similar phase. The directional spectrum

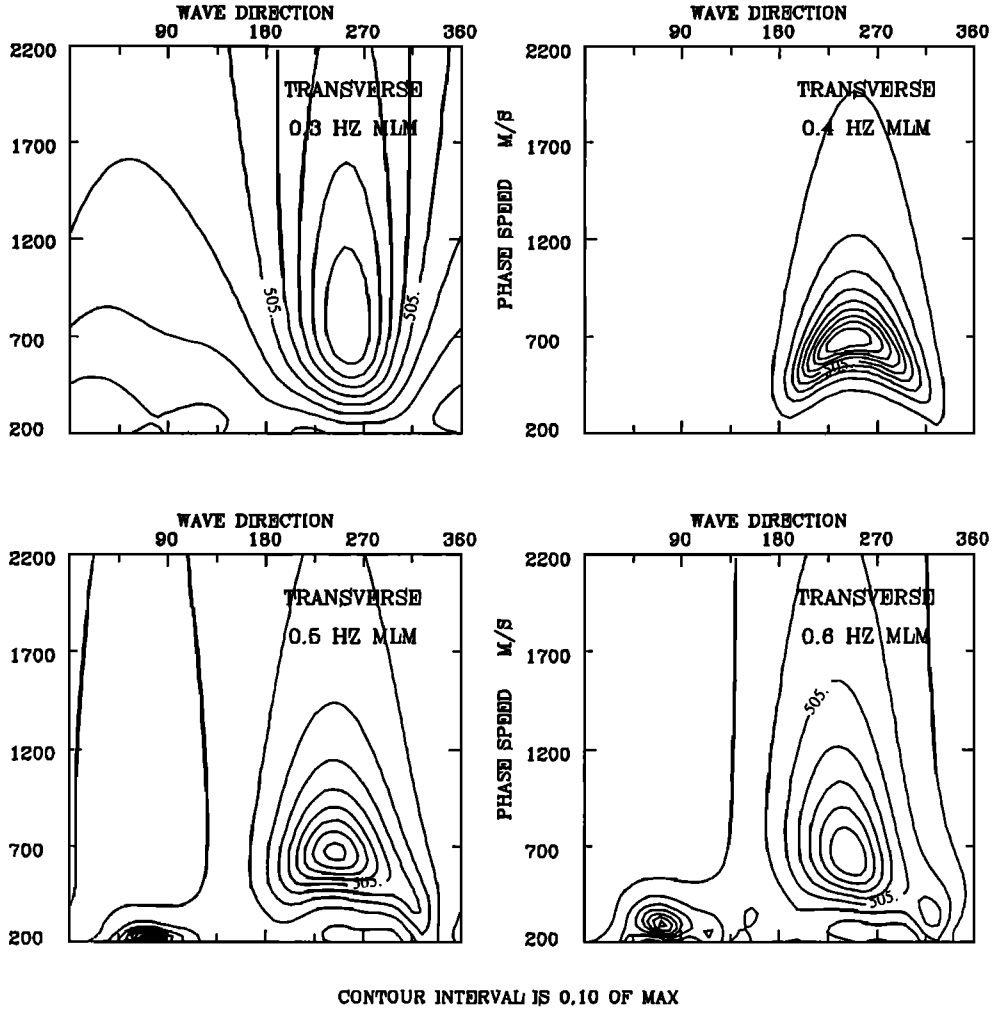

Figure 22. Double-frequency directional spectra estimation from the transverse seismometer four-point array using the maximum likelihood method during the 30-minute data set beginning at November 29, 1130 UT for frequency bands centered at 0.3, 0.4, 0.5, and 0.6 Hz, respectively, from upper left to lower right.

of the double-frequency energy was found using the four-point array with the maximum likelihood method. Various data sets were analyzed to confirm Longuet-Higgins' theory which proposes that the propagation direction of double-frequency microseisms occurs in the direction of the vector sum of the opposing single-frequency seas.

Acknowledgments. This work was supported under several Office of Naval Research contracts between 1990 and 1993 in the sections of Ocean Acoustics and Geology and Geophysics. I would also like to thank the staff of the Field Research Facility of the Army Corps of Engineers in Duck, North Carolina, headed by Bill Berkemeyer and the crew of the R/V *Cape Henlopen* out of the University of Delaware.

References

Goodman, D., Analysis and observations of spatially coherent seafloor microseisms, Ph.D. dissertation, Univ. of Miami, Fla., 1990.

Herbers, T., and R. Guza, Wind-wave nonlinearity observed at the seafloor, I, Forced-wave energy, *J. Phys. Oceanogr.*, *21*, 1740–1761, 1991.

Herbers, T., and R. Guza, Veering winds, directionally opposing seas, and double-frequency pressure fluctuations at the sea floor, *J. Acoust. Soc. Am.*, *91*(4), 2345, 1992.

Longuet-Higgins, M. S., A theory of the origin of microseisms, *Philos. Trans. R. Soc. London, A*, *A243*, 1, 1950.

Miche, M., Movements Ondulatores de la Mer en Profoundeur Constante ou Decroissante, *Ann. Ponts. Chaussées*, *114*, 25–406, 1944.

Nye, T., Measurements of the directional spectra of surface gravity waves and seafloor microseisms using a pressure sensor and two buried horizontal seismometers, Ph.D. dissertation, Univ. of Miami, Fla., 1992.

Nye, T., and T. Yamamoto, Field test of the Buried Ocean Wave Directional Spectrometer (BOWDS) System, *J. Waterw., Port Coastal Ocean Eng.*, in press, 1994.

Young, I. R., S. Hasselman, and K. Hasselman, Computations of the response of a wave spectrum to a sudden change in wind direction, *J. Phys. Oceanogr.*, *17*, 1317–1338, 1987.

T. Nye and T. Yamamoto, Division of Applied Marine Physics, RSMAS, University of Miami, 4600 Rickenbacker Causeway, Miami, FL 33149.

(Received August 31, 1993; revised December 2, 1993; accepted February 1, 1994.)